

Research Article

Different Statistical Modeling to Predict Compressive Strength of High-Strength Concrete Modified with Palm Oil Fuel Ash

Soran Abdrahman Ahmad^{1,*} , Bilal Kamal Mohammed² , Serwan Khwrshid Rafiq¹ , Brwa Hama Saeed¹ ,
Kawa Omar Fqi³ 

¹ Civil Engineering Department, Collage of Engineering, University of Sulaimani, Sulaymaniyah, 46001, Iraq

² Sulaimani Technical Institute, Sulaimani Polytechnic University, Sulaymaniyah, 46001, Iraq

³ Qaiwan Company, Salim Street, Sulaimaniyah,, 46001, Iraq

*Corresponding Author: Soran Abdrahman Ahmad, E-mail: Soran.abdrahman@univsul.edu.iq

Article Info	Abstract
Article History	The present study focuses on proposing various statistical models, such as linear regression (LR), nonlinear regression (NLR), and artificial neural network (ANN), to forecast the compressive strength of environmentally friendly high-strength concrete, incorporating waste agricultural material like palm oil fuel ash (POFA). A dataset of 105 experimental observations was compiled from existing literature to achieve this goal, which was subsequently partitioned into training and testing subsets. Each model was developed based on the training data and evaluated using the testing data. The performance of each proposed model was gauged using diverse statistical metrics like the coefficient of determination, mean absolute error, root mean square error, and scatter index to identify the most effective model. The findings indicate that using POFA with a finer particle size exerts a greater influence on the concrete's properties. The replacement was done using the weight method, and the predicted equation worked with the variation of the used rate of POFA from 0 to 60% of total binder weight. Substituting a portion of cement with POFA leads to a reduction in the heat of hydration and an extension of the setting time. The optimal percentage of POFA is 30%, yielding mechanical properties superior to those of the control mixture, particularly in the later stages of development. Among the models considered, the ANN demonstrates superior efficiency and accuracy in predicting the compressive strength of conventional concrete modified with POFA compared to LR and NLR models. This is evident in the ANN's higher R2 values of 52% and 16%, respectively, and a lower scatter index below 0.1%.
Received Mar 29, 2024	
Revised Apr 18, 2024	
Accepted Apr 19, 2024	
Keywords	
Metal straps	
Palm Oil Fuel Ash	
Bending	
Strengthening	Normal
Concrete	



Copyright: © 2024 Soran Abdrahman Ahmad, Bilal Kamal Mohammed, Serwan Khwrshid Rafiq, Brwa Hama Saeed Hamah Ali and Kawa Omer Faqi. This article is an open-access article distributed under the terms and conditions of the Creative Commons Attribution (CC BY 4.0) license.

1. Introduction

High-strength concrete is characterized by a similar mixture composition to normal concrete, albeit with smaller aggregates, a lower water-to-binder ratio, and the incorporation of superplasticizers to regulate concrete workability. Additionally, supplementary cementitious materials are utilized in conjunction with

cement to mitigate environmental impacts and promote pozzolanic reactions resulting from these applications [4].

Researchers have conducted numerous experiments involving the utilization of palm oil shells as lightweight aggregate concrete [21- 25]. Alternatively, a more viable approach with added benefits involves the combustion of Palm oil husk and kernel shell in a controlled environment within a thermal power plant [26, 27]. The resulting product of the combustion process is known as palm oil fuel shell (POFS), with an annual production exceeding 0.1 million tons in Thailand alone [28, 29].

According to ASTM C618, a material with $\text{SiO}_2 + \text{Al}_2\text{O}_3 + \text{Fe}_2\text{O}_3 > 70\%$ in its composition qualifies as pozzolanic material [29, 30], for that and based on the chemical compositions provided by Hamada et al [20], palm oil fuel ash is deemed to be pozzolanic material, that leading to the formation of an additional gel of calcium silicate hydroxide crucial for enhancing compressive strength.

The pozzolanic nature of POFA has spurred numerous research endeavors focusing on its utilization as a partial substitute for cement in concrete, with investigations into its impact on the fresh and mechanical properties of various concrete types [31-33]. Hussin et al [9] conducted a study on incorporating POFA as a 20% partial replacement for cement, examining two distinct curing periods (75 and 90 days). The outcomes revealed that the compressive strength of the modified mixture surpassed that of the control concrete by 1.7% after 75 days of curing and by 3.8% after 90 days of curing.

Sata et al [34] examined the utilization of POFA as a partial substitute for cement at varying rates (0, 10, 20, and 30%) and different curing durations (7, 28, 60, and 90 days). They observed that employing 10 and 20% of POFA as a partial replacement for cement at early stages resulted in greater compressive strength than the control mixture. Conversely, the mixture containing 30% of POFA exhibited strength equivalent to the control mix. However, at later stages (i.e., 28, 60, and 90 days), all mixtures incorporating POFA demonstrated superior strength compared to the control mix.

In a similar vein, Tangchirapat et al [35] investigated the incorporation of POFA as a partial substitute for cement at various rates (0, 10, 20, and 30%) and different curing periods (7, 28, and 90 days). Their findings indicated that utilizing 10% of POFA as a partial replacement for cement during the early stages led to higher compressive strength than the control mix. Conversely, mixtures containing 20% and 30% of POFA exhibited lower strength than the control mix. Nevertheless, at later stages (i.e., 28 and 90 days), all mixtures incorporating POFA showcased superior strength compared to the control mix.

Johari et al. [36] conducted an investigation into the utilization of POFA as a partial substitute for cement at varying rates (0%, 20%, 40%, and 60%) and different curing periods (1, 3, 7, and 28 days). The results indicated that, in the early stages (1 and 3 days), all mixtures containing palm oil fuel ash exhibited decreased compressive strength compared to the control mixture. However, after 7 days of curing, the mix with 20% POFA as a partial cement replacement showed higher compressive strength than the control.

Furthermore, by the 28th day of curing, all POFA mixes demonstrated superior strength compared to the control mix.

Extensive research suggests that incorporating 30% POFA as a partial cement replacement in high-strength concrete yields optimal effects on concrete properties, especially when using POFA with finer particles exhibiting higher pozzolanic activity. This study proposes various models, such as linear, nonlinear regression, and ANN, to forecast the compressive strength of high-strength concrete (HSC) when modified with POFA as a partial cement replacement. The efficacy of these models is evaluated through statistical parameters like coefficient of determination, mean absolute error, root mean square error, and scatter index to identify the most effective models for predicting compressive strength with the selection of the most efficient models for the compressive strength of high strength concrete which modified with POFA can be predicted with high accuracy without waiting for the trail mix curing time, which reduce the waiting and spending the time.

2. Research significant

This paper addresses the development of a numerical framework to predict the compressive strength of high-strength concrete. The study examines the influence of various factors such as POFA, silica fume content, water-to-binder ratio (w/b), cement content, sand content, gravel, superplasticizer, and curing time on the compressive strength of HSC through LR, NLR, and ANN models. This novel approach aims to identify the most reliable model using statistical parameters while reducing the waiting time of trail mix to find the effect of used POFA on the compressive strength of the concrete mix. Furthermore, statistical analysis is conducted for each independent variable to determine the optimal palm oil ratio that positively impacts the properties of HSC.

3. Methodology

As in Figure 1, the methodology utilized involved the statistical analysis of the collected data in Table 1 for each independent variable. The relationship between the independent parameters (w/b which is water to-binder ratio, cement content (CC), Palm oil fuel ash content (POFA), Silica fume content (SF), Sand content (SC), gravel content (GC), superplasticizer content (SP), and curing time (T)) and the measured compressive strength was established. Subsequently, the collected data was divided into training and testing sets, and models were developed based on the independent variables. These proposed models were then scrutinized for their efficacy through statistical parameters. The model demonstrating the highest efficiency, as determined by the statistical parameters, was chosen to forecast the compressive strength of High-Strength Concrete (HSC) enhanced with palm oil fuel ash.

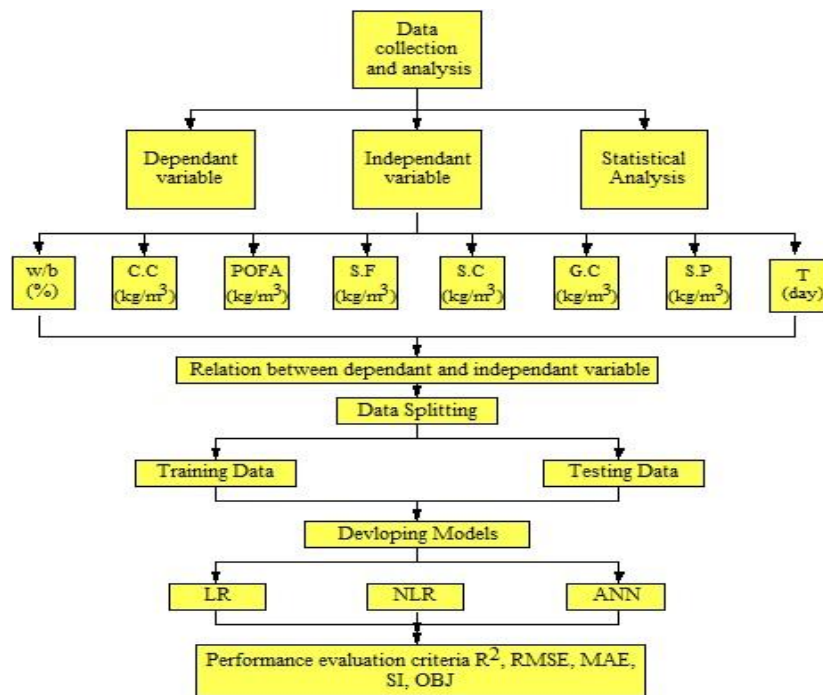


Figure 1. Methodology steps

4. Statistical Analysis

In this section, we have presented comprehensive details regarding the related data, encompassing the expression of gathered information, necessary statistical analyses, graphical representations, and the utilization of various predictive models for estimating compressive strength. Additionally, we have included all independent parameters that are utilized within these models.

4.1. Data Collections

Based on various experimental studies documented in the literature, 104 data points have been gathered and are presented in Table 1 below. This dataset encompasses all pertinent independent variables (such as w/b ratio, cement content, palm oil fuel ash, silica fume content, coarse aggregate, fine aggregate, superplasticizer dosage (SP), and curing time) necessary for predicting the dependent variable, compressive strength.

Table 1. Experimental data collected from the literature

Ref.	w/b	Cement Content (kg/m ³)	Powder Palm Oil (kg/m ³)	Silica Fume (kg/m ³)	Sand Content (kg/m ³)	Coarse Aggregate Content (kg/m ³)	SP Content (kg/m ³)	Curing Time (Days)	Compressive Strength (MPa)
[9]	0.435	400	0	0	678.7	1090	0	75	55
	0.435	320	80	0	678.7	1090	0	75	56
	0.435	400	0	0	678.7	1090	0	90	56.65
	0.435	320	80	0	678.7	1090	0	90	58.89
[34]	0.28	560	0	0	764	981	7.9	7	68.8
	0.28	532	0	28	760	975	10.2	7	71.1

0.28	504	0	56	755	970	12.4	7	77.5	
0.28	476	0	84	751	964	14.7	7	75.9	
0.28	504	56	0	757	971	8.5	7	71.7	
0.28	448	112	0	749	962	11.8	7	71.1	
0.28	392	168	0	742	952	16.9	7	68.5	
0.28	560	0	0	764	981	7.9	28	77.5	
0.28	532	0	28	760	975	10.2	28	80.2	
0.28	504	0	56	755	970	12.4	28	91.7	
0.28	476	0	84	751	964	14.7	28	92.6	
0.28	504	56	0	757	971	8.5	28	81.3	
0.28	448	112	0	749	962	11.8	28	85.9	
0.28	392	168	0	742	952	16.9	28	79.8	
0.28	560	0	0	764	981	7.9	60	83.8	
0.28	532	0	28	760	975	10.2	60	85.2	
0.28	504	0	56	755	970	12.4	60	96.7	
0.28	476	0	84	751	964	14.7	60	95	
0.28	504	56	0	757	971	8.5	60	86.5	
0.28	448	112	0	749	962	11.8	60	88.5	
0.28	392	168	0	742	952	16.9	60	84.7	
0.28	560	0	0	764	981	7.9	90	87.5	
0.28	532	0	28	760	975	10.2	90	88	
0.28	504	0	56	755	970	12.4	90	97.9	
0.28	476	0	84	751	964	14.7	90	96	
0.28	504	56	0	757	971	8.5	90	89.1	
0.28	448	112	0	749	962	11.8	90	91.5	
0.28	392	168	0	742	952	16.9	90	88.7	
0.32	550	0	0	760	968	6.4	7	54.9	
0.32	495	55	0	753	959	6.8	7	55.6	
0.32	440	110	0	745	950	8.6	7	54.6	
0.32	385	165	0	738	940	11.6	7	53.2	
0.32	550	0	0	760	968	6.4	28	58.5	
0.32	495	55	0	753	959	6.8	28	59.5	
0.32	440	110	0	745	950	8.6	28	60.9	
0.32	385	165	0	738	940	11.6	28	58.8	
[35]	0.32	550	0	0	760	968	6.4	90	64.7
0.32	495	55	0	753	959	6.8	90	67.5	
0.32	440	110	0	745	950	8.6	90	69.4	
0.32	385	165	0	738	940	11.6	90	66.1	
0.32	550	0	0	760	968	6.4	180	68.5	
0.32	495	55	0	753	959	6.8	180	72	
0.32	440	110	0	745	950	8.6	180	73.7	
0.32	385	165	0	738	940	11.6	180	69	

	0.27	550	0	0	741.2	1033.6	12.1	1	63
	0.27	440	110	0	741.2	1033.6	12.1	1	44
	0.27	330	220	0	741.2	1033.6	12.1	1	35
	0.27	220	330	0	741.2	1033.6	12.1	1	25
	0.27	550	0	0	741.2	1033.6	12.1	3	79
	0.27	440	110	0	741.2	1033.6	12.1	3	72
	0.27	330	220	0	741.2	1033.6	12.1	3	66
[36]	0.27	220	330	0	741.2	1033.6	12.1	3	50
	0.27	550	0	0	741.2	1033.6	12.1	7	86
	0.27	440	110	0	741.2	1033.6	12.1	7	86
	0.27	330	220	0	741.2	1033.6	12.1	7	83
	0.27	220	330	0	741.2	1033.6	12.1	7	80
	0.27	550	0	0	741.2	1033.6	12.1	28	91
	0.27	440	110	0	741.2	1033.6	12.1	28	98
	0.27	330	220	0	741.2	1033.6	12.1	28	103
	0.27	220	330	0	741.2	1033.6	12.1	28	98
	0.27	550	0	0	742.5	1034	12.1	90	100
[37]	0.27	440	110	0	742.5	1034	12.1	90	105
	0.27	330	220	0	742.5	1034	12.1	90	107
	0.27	220	330	0	742.5	1034	12.1	90	106
	0.18	500	0	0	797	1195	5	7	42
	0.18	450	50	0	797	1195	5	7	45
	0.18	400	100	0	797	1195	5	7	48
[38]	0.18	350	150	0	797	1195	5	7	47
	0.18	500	0	0	797	1195	5	28	66
	0.18	450	50	0	797	1195	5	28	67
	0.18	400	100	0	797	1195	5	28	70
	0.18	350	150	0	797	1195	5	28	69
	0.27	550	0	0	742	1033	12.1	1	66
	0.27	440	110	0	742	1033	12.1	1	44.8
	0.27	330	220	0	742	1033	12.1	1	36.4
	0.27	220	330	0	742	1033	12.1	1	26
	0.27	550	0	0	742	1033	12.1	3	79.2
	0.27	440	110	0	742	1033	12.1	3	73.7
[39]	0.27	330	220	0	742	1033	12.1	3	66.7
	0.27	220	330	0	742	1033	12.1	3	50.3
	0.27	550	0	0	742	1033	12.1	7	87
	0.27	440	110	0	742	1033	12.1	7	87
	0.27	330	220	0	742	1033	12.1	7	85
	0.27	220	330	0	742	1033	12.1	7	79
	0.27	550	0	0	742	1033	12.1	28	91.6
	0.27	440	110	0	742	1033	12.1	28	99.6

0.27	330	220	0	742	1033	12.1	28	101
0.27	220	330	0	742	1033	12.1	28	98.1
0.27	550	0	0	742	1033	12.1	90	100.6
0.27	440	110	0	742	1033	12.1	90	105
0.27	330	220	0	742	1033	12.1	90	110
0.27	220	330	0	742	1033	12.1	90	108.6
0.27	550	0	0	742	1033	12.1	180	105
0.27	440	110	0	742	1033	12.1	180	108.5
0.27	330	220	0	742	1033	12.1	180	114.5
0.27	220	330	0	742	1033	12.1	180	112
0.27	550	0	0	742	1033	12.1	360	106
0.27	440	110	0	742	1033	12.1	360	112
0.27	330	220	0	742	1033	12.1	360	116.5
0.27	220	330	0	742	1033	12.1	360	115

4.2. Statistical Analysis

Histogram distributions have been meticulously crafted to visualize the data distribution for each independent parameter listed in Table 1. The resultant findings have been effectively integrated into these histograms following a thorough statistical analysis. Each independent parameter, including the water-to-binder ratio (w/b), cement content, palm oil fuel ash (POFA), silica fume content, sand content, gravel content, superplasticizer dosage, and curing time, has been individually scrutinized concerning the dependent parameter, compressive strength. These relationships have been meticulously illustrated and elucidated in detail across Figures 2 through 17. These relations have been drawn to find the effect of each independent variable separately on compressive strength and to show the statistical distribution for independent variables.

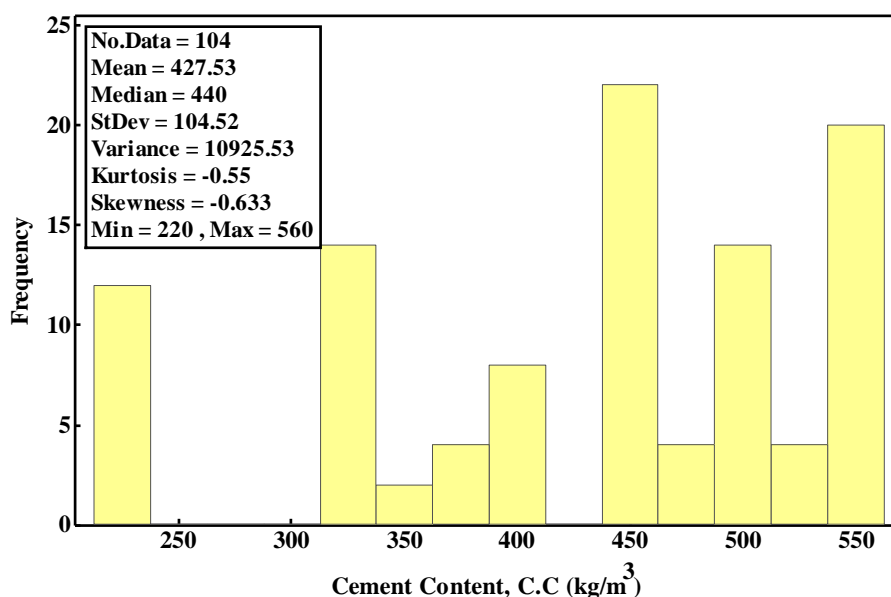


Figure 2. Water to binder ratio histogram

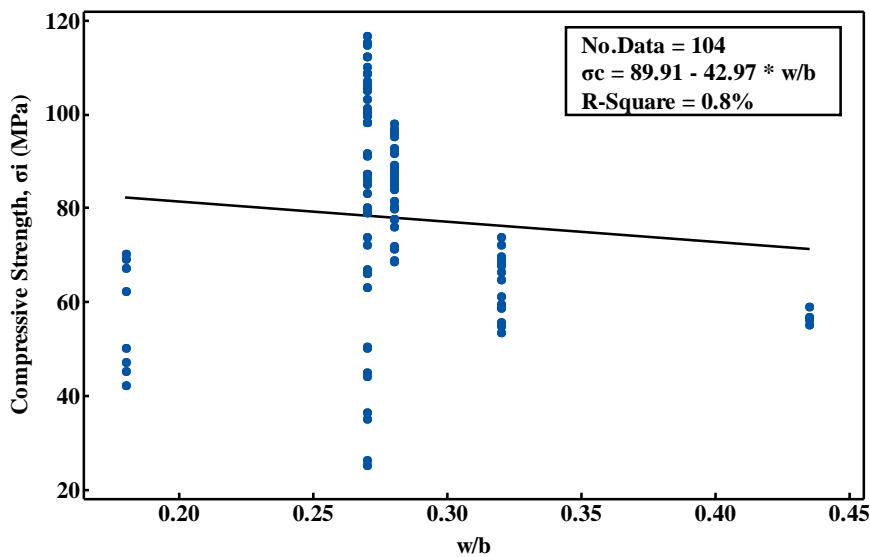


Figure 3. Scatter relation between w/b and compressive strength (MPa)

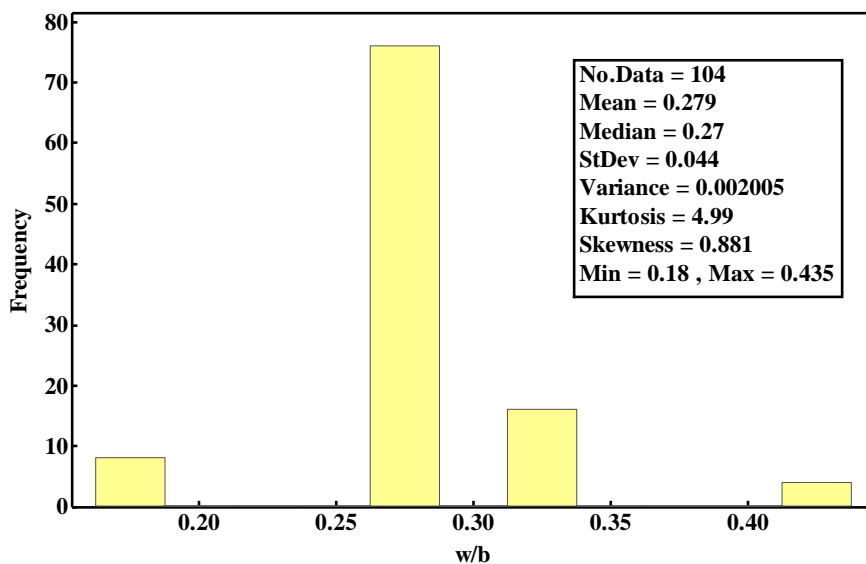


Figure 4. Cement content (kg/m³) histogram

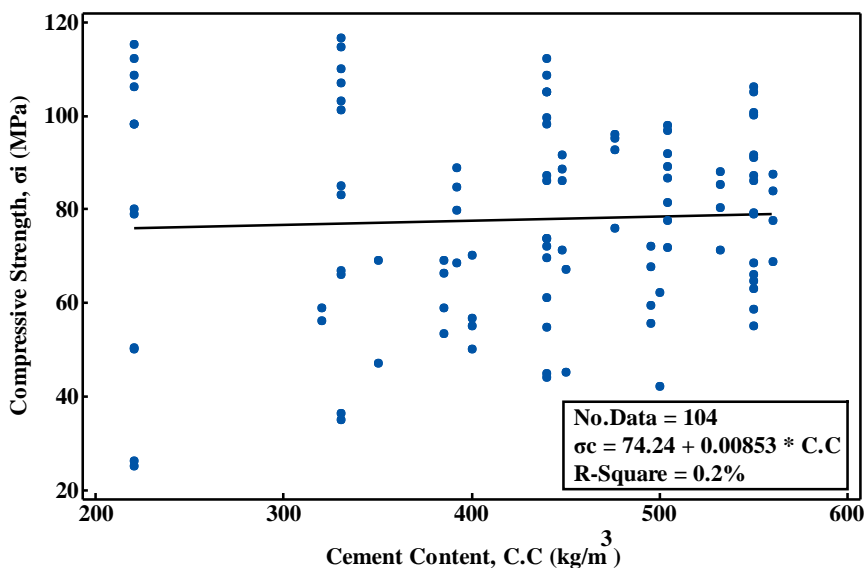


Figure 5. Scatter relation between cement content and compressive strength (MPa)

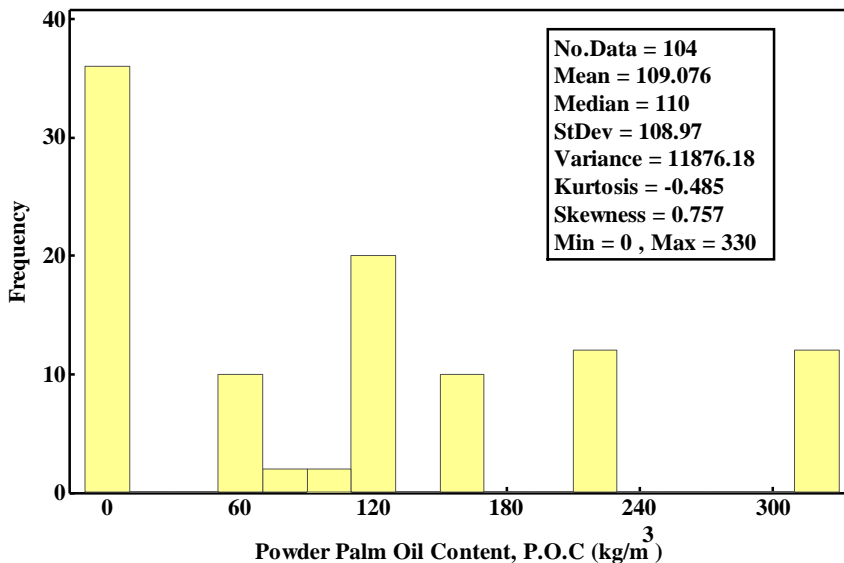


Figure 6. Palm oil fuel ash content (kg/m³) histogram

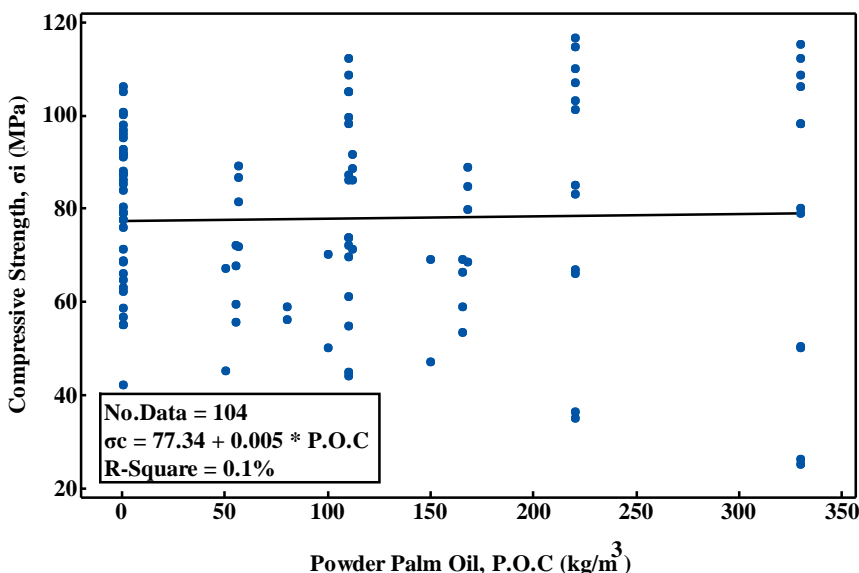


Figure 7. Scatter relation between POFA content and compressive strength

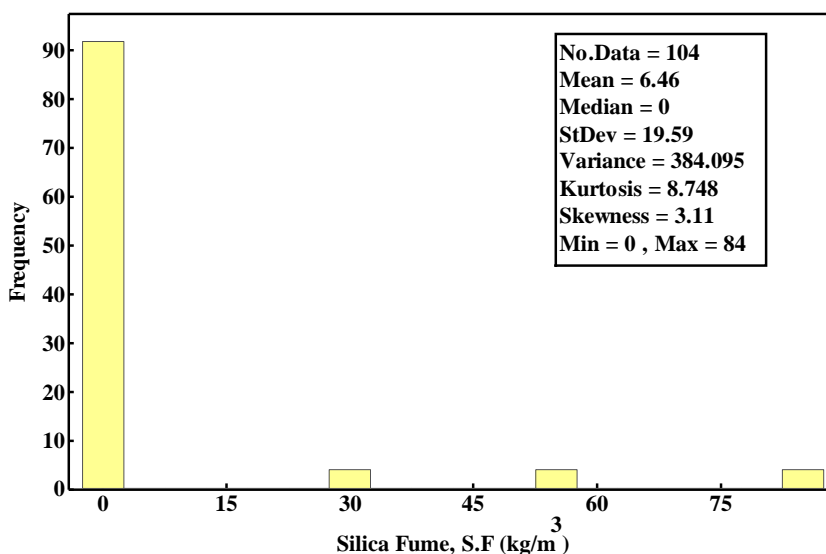


Figure 8. Silica fume content (kg/m³) histogram

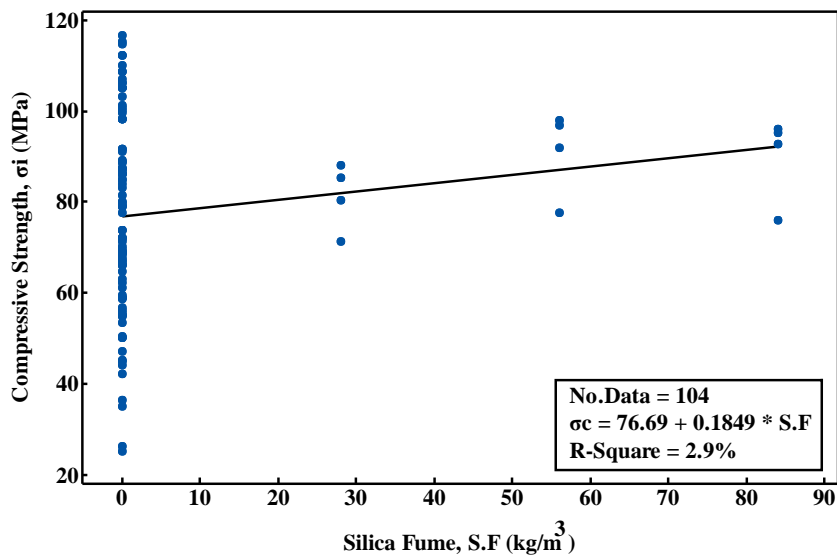


Figure 9. Scatter silica fume content (kg/m^3) and compressive strength

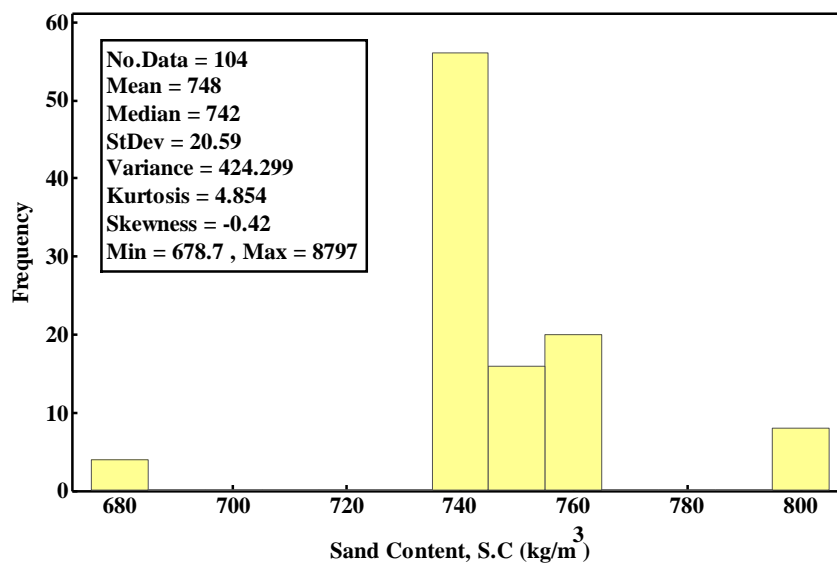


Figure 10. Sand content (kg/m^3) histogram

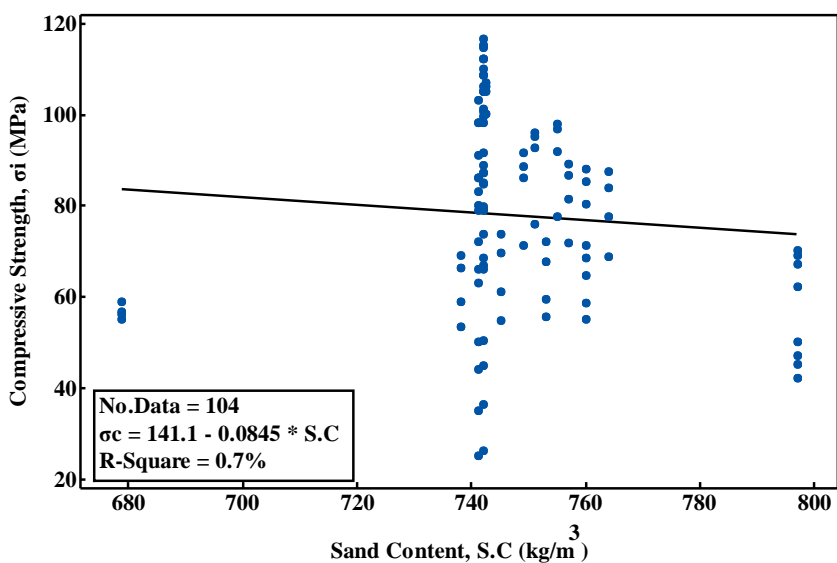


Figure 11. Scatter relation between sand content (kg/m^3) and compressive strength

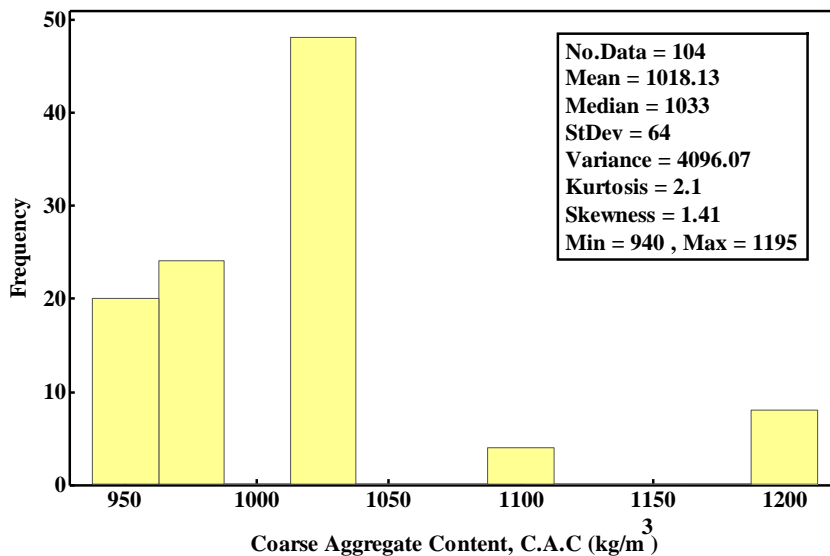


Figure 12. Coarse aggregate content (kg/m³) histogram

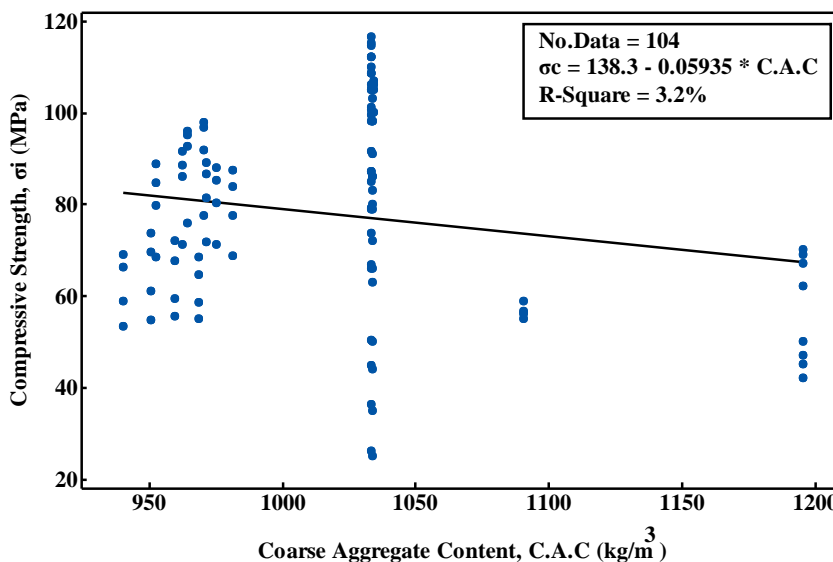


Figure 13. Scatter relation between coarse aggregate content and compressive strength

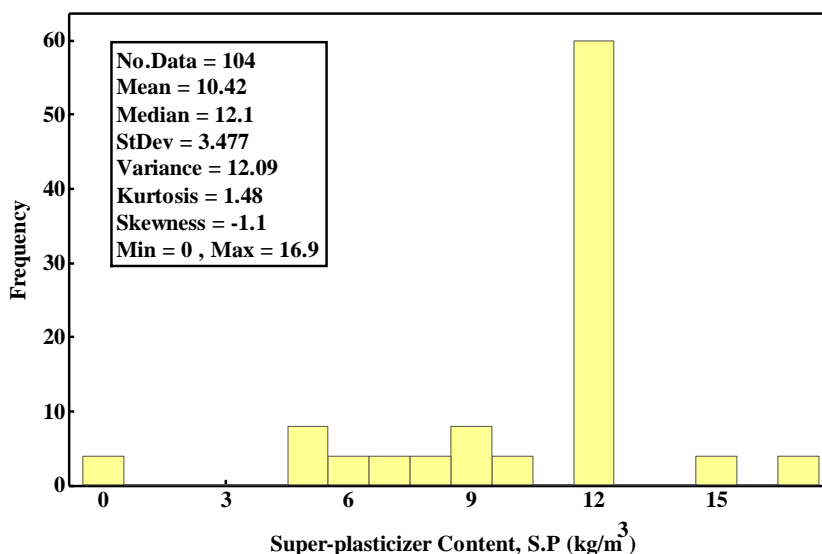


Figure 14. Superplasticizer content (kg/m³) histogram

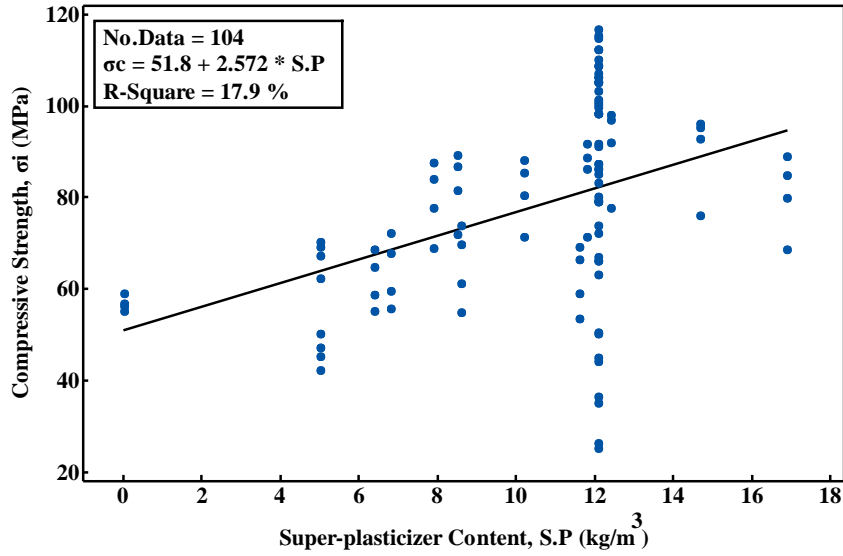


Figure 15. Scatter relation between supper-plasticizer content and compressive strength

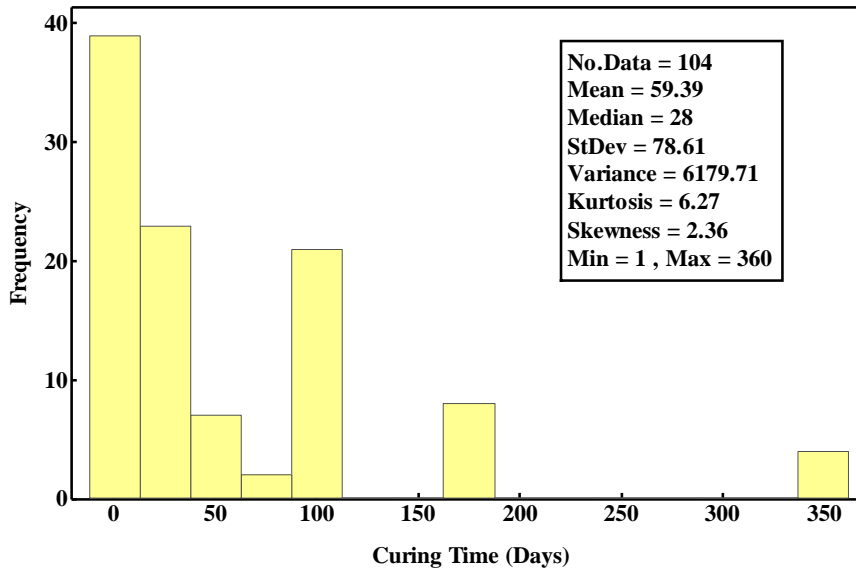


Figure 16. Curing time (Days) histogram

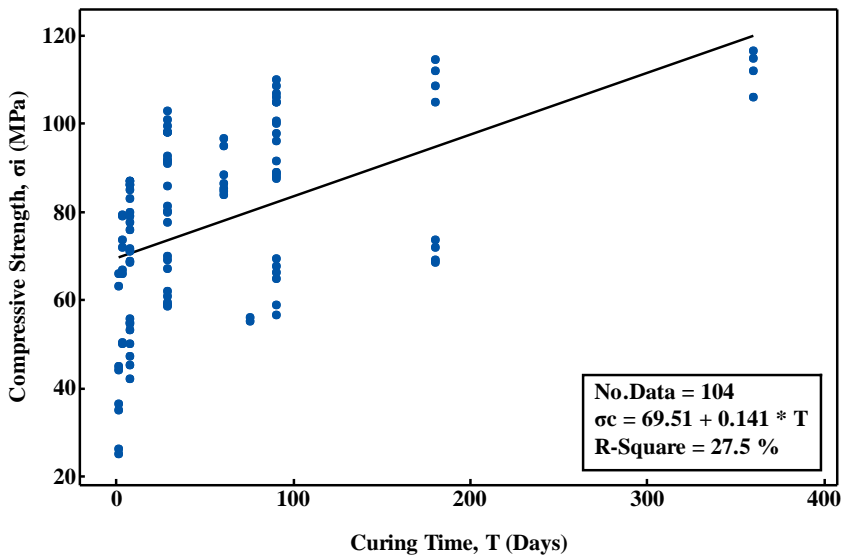


Figure 17. Scatter relation between curing time (Days) and compressive strength

4.3 Modeling

The dataset presented in Table 1 has served as the foundation for developing several predictive models designed to estimate the compressive strength of high-strength concrete that has been enhanced with palm oil fuel ash. Considering various factors and parameters, these models have been meticulously crafted to provide accurate and reliable predictions regarding the compressive strength of such modified concrete compositions. Through a rigorous analysis of the collected data and incorporating pertinent variables, these models offer valuable insights into the performance and behavior of high-strength concrete formulations incorporating palm oil fuel ash as a modifying agent.

4.3.1 Linear Regression (LR)

Its application in engineering allows for the prediction of compressive strength, following the format outlined below:

$$\sigma_{cp} = a \pm b * \left(\frac{w}{b}\right) \pm c * (C.C) \pm d * (POFA) \pm e * (S.F) \pm f * (S.C) \pm g * (G.C) \pm h * (S.P) \pm i * (T) \quad (1)$$

Where w/b is water to binder ratio, CC is cement content (kg/m³), POFA is palm oil fuel ash content (kg/m³), SF is silica fume content (kg/m³), SC is sand content (kg/m³), C.A is coarse aggregate content (kg/m³), SP is super plasticizer content (kg/m³), and T is curing time (days) while a, b, c, d, e, f, g, h, and i are model parameters.

4.3.2 Nonlinear regression (NLR)

This model finds applicability in predicting the compressive strength of high-strength concrete, employing parameters dependent on it, as demonstrated in the following format:

$$\sigma_{cp} = a * \left(\frac{w}{b}\right)^b \pm c * (C.C)^d \pm e * (POFA)^f \pm g * (S.F)^h \pm i * (S.A)^j \pm k * (G.C)^l \pm m * (S.P)^n \pm o * (T)^p \quad (2)$$

Where w/b is water to binder ratio, CC is cement content (kg/m³), POFA is palm oil fuel ash content (kg/m³), SF is silica fume content (kg/m³), SC is sand content (kg/m³), C. A is coarse aggregate content (kg/m³), SP is super plasticizer content (kg/m³), and T is curing time (days) while a, b, c, d, e, f, g, h, i, j, k, l, m, n, o and p are models parameters.

4.3.3 Artificial Neural Network (ANN)

The Weka software package implemented the ANN model, specifically version 3.8.5. Artificial Neural Networks (ANN) are recognized for their reliability, mimicking the human brain's functionality, with components including input, hidden, and output layers. Unlike conventional models, ANN lacks a fixed structure, with the analytical process contingent upon the input parameters and the nature of the problem at hand, as illustrated in Figure 18 below.

4.4 Models Assessment

For the gathered data, three distinct models have been put forth (Linear, non-linear regression, ANN), and their efficacy is assessed based on several parameters outlined in equations 3 to 7. Models with higher coefficient of determination (R^2), lower root mean square error (RMSE), and mean absolute error (MAE) are deemed more dependable.

According to the statistical criteria utilized, a higher R^2 value is preferred. SI greater than 0.3 indicates poor performance, while values between 0.2 and 0.3 are acceptable. SI values between 0.1 and 0.2 indicate good performance, whereas an SI less than 0.1 signifies excellent performance, as detailed in reference [44].

$$R - square = 1 - \frac{\sum(Y_i - Y_p)^2}{\sum(Y_i - Mean)^2} \quad (3)$$

$$RMSE = \sqrt{\frac{\sum(Y_i - Y_p)^2}{N}} \quad (4)$$

$$SI = \frac{RMSE}{Mean} * 100 \quad (5)$$

$$MAE = \frac{\sum(Y_i - Y_p)}{n} \quad (6)$$

$$OBJ = \left(\frac{N.Traial}{N.Total}\right) * \left(\frac{RMSE_{Traial} + MAE_{Traial}}{R^2_{Traial} + 1}\right) + \left(\frac{N.Testing}{N.Total}\right) * \left(\frac{RMSE_{Testing} + MAE_{Testing}}{R^2_{Testing} + 1}\right) \quad (7)$$

5. Results and Discussions

5.1 Linear Regression

The collected dataset was partitioned into training and testing data subsets following the analysis procedure. Using the training data comprising 79 observations, Equation 8 was derived and subsequently evaluated using the testing data set of 26 observations. Figure 18 illustrates the relationship between the actual compressive strength of high-strength concrete modified with palm oil fuel ash and the predicted compressive strength values for the same mixture, elucidating the efficacy of the obtained equation.

Equation 8 indicates that the water-to-binder ratio, sand content, and gravel content negatively influence the compressive strength, whereas the superplasticizer content and curing time exhibit the most significant positive impact on compressive strength. Furthermore, as detailed in the analysis, the effect of silica fume, cement content, and POFA follow in terms of their positive influence on compressive strength.

$$\sigma P = 86.56 - 77.57 * w/b + 0.025 * C.C + 0.0017 * POFA + 0.075 * S.F - 0.04 * S.C - 0.001 * G.C + 2.3 * S.P + 0.134 * T \quad (8)$$

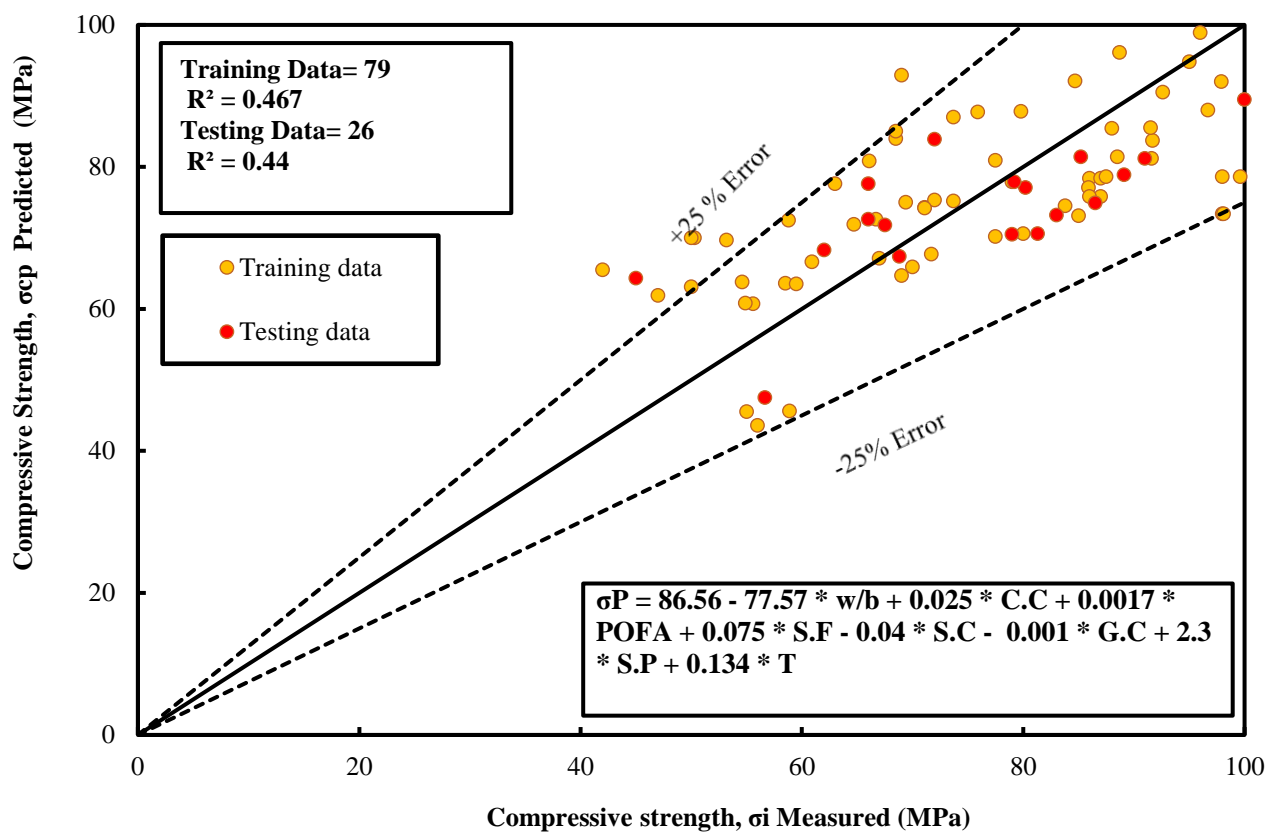


Figure 18. Correlation between measured compressive strength and predicted compressive strength using linear regression

5.2 Nonlinear Regression

Due to the potential nonlinearity in the relationship between the compressive strength (dependent parameter) and various independent parameters (water-to-binder ratio, cement content, palm oil fuel ash content, silica fume content, superplasticizer content, fine aggregate content, coarse aggregate content, and curing time), a nonlinear model has been employed to formulate the model. Using a dataset consisting of 79 entries, Equation 9 has been derived and subsequently tested against a separate testing dataset comprising 26 entries. Figure 19 depicts the correlation between the measured compressive strength and the predicted compressive strength obtained from Equation 9, showcasing the model's efficacy. Analysis of Equation 9 reveals that the water-to-binder ratio exerts the most significant negative influence on compressive strength, followed by the proportions of sand and gravel. Conversely, curing time exhibits the most notable positive impact on compressive strength values.

$$\begin{aligned} \sigma P = & -597.7 * w/b^{1.58} + 0.001 * C.C^{1.554} + 0.001 * POFA^{0.001} + 11.07 * S.F^{0.001} - 0.005 * S.C^{1.72} \\ & - 0.001 * G.C - 0.554 + 21.1 * S.P^{0.001} + 26.6 * T^{0.2} \end{aligned} \tag{9}$$

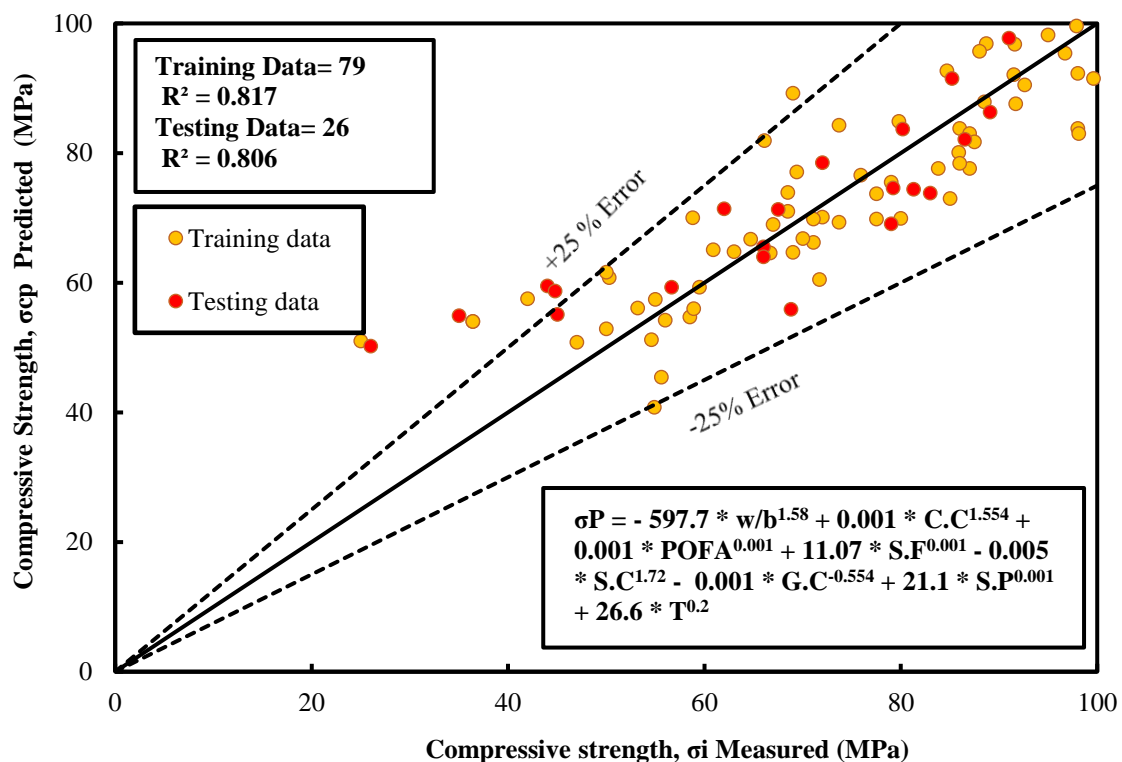


Figure 19. Correlation between measured compressive strength and predicted compressive strength using non-linear regression

5.3 ANN

One aim of this research was to improve the Artificial Neural Network (ANN) performance by exploring various parameters such as the number of hidden layers, neurons, momentum, learning rate, and iteration numbers. The goal was to identify the optimal configuration to generate the most precise forecasts for the compressive strength of high-strength concrete mixtures containing palm oil fuel ash. Researchers assessed the ANN model's effectiveness by utilizing distinct training and testing datasets to predict compressive strength values based on specified input parameters. These forecasts were compared against experimentally determined compressive strengths of regular concrete mixtures incorporating palm oil fuel ash. Analysis indicated that the ANN model surpassed other developed models in accuracy. Figure 20 compares experimentally determined compressive strength values and those computed by the ANN model for high-strength concrete modified with palm oil fuel ash in the training and testing datasets. The study illustrates that when configured with optimized parameters, the ANN model can predict the compressive strength of high-strength concrete modified with palm oil fuel ash with an error margin of $\pm 20\%$, whereas other models exhibited errors within $\pm 25\%$. Although ANN-based models are highly effective for construction applications, a significant drawback is their opaque nature, limiting users' ability to interpret the model's internal mechanisms without conducting numerous trials.

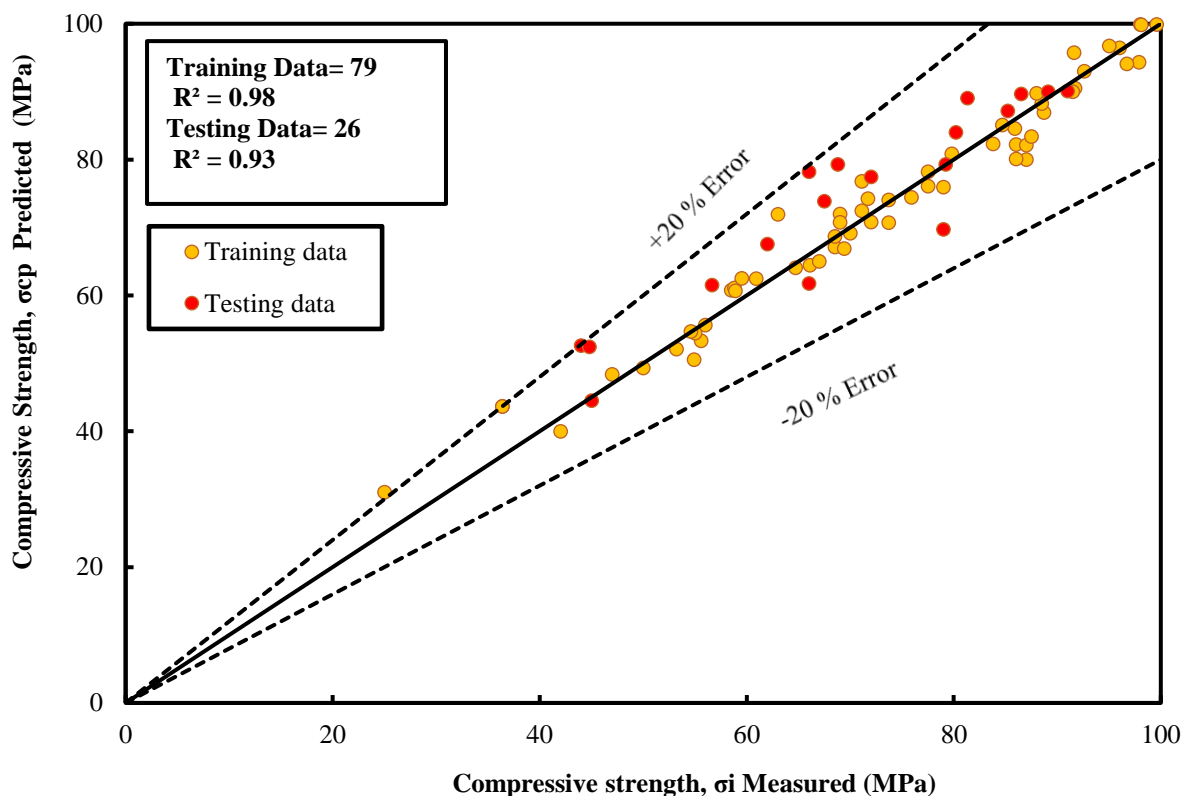


Figure 20. Correlation between measured compressive strength and predicted compressive strength using ANN

5.4 Models Assessment

According to the findings outlined in Table 2, the ANN model stands out as the most effective and trustworthy among the tested models. It exhibits a notably high coefficient of determination (R^2) compared to others and demonstrates lower root mean square and lower mean absolute error. Furthermore, the range of values for the SI falls between 0 and 0.1 for both training and testing datasets, indicating the exceptional performance of the proposed model.

Table 2. Assessment tools value for proposed models

Models	LR		NLR		ANN	
	Training	Testing	Training	Testing	Training	Testing
R^2	0.467	0.44	0.817	0.806	0.98	0.93
RMSE (MPa)	15.01	17.371	8.789	10.217	4.88	6.5
MAE (MPa)	12.146	13.219	6.958	8.606	3.11	5.01
SI	0.19	0.23	0.112	0.136	0.06	0.09
OBJ	23.09	-----	9.92	-----	6.21	-----

6. Conclusions

Following an extensive examination of 105 data points on the integration of palm oil fuel ash in High Strength Concrete (HSC) as a cement alternative and the development of three distinct models, several conclusions were drawn: The Artificial Neural Network (ANN) model outperformed the Linear Regression (LR) and Non-linear Regression (NLR) models in predicting the compressive strength of high-strength concrete. The ANN model showed superiority with higher values of the coefficient of determination (R^2) and lower values of Root Mean Square Error (RMSE), Objective Function (OBJ), Scatter Index (SI), and Mean Absolute Error (MAE). Using statistical assessment tools, the models were ranked from least to most suitable: the LR model, due to its highest scatter index and lowest R^2 values; the NLR model; and the ANN model as the most suitable and superior performer. Analysis indicated that the water-to-binder ratio is the most significant factor influencing the compressive strength of high-strength concrete. Incorporating palm oil fuel ash as a partial cement replacement reduces the heat of hydration and extends the setting time. The optimal percentage of palm oil fuel ash for use in concrete, without compromising mechanical properties, is determined to be 30%.

Declaration of Competing Interest: The authors declare they have no known competing interests.

References

- [1] Abutaha, F., Razak, H. A., Ibrahim, H. A., & Ghayeb, H. H. (2018). Adopting particle-packing method to develop high strength palm oil clinker concrete. *Resources, conservation and Recycling*, 131, 247-258.
- [2] Philip, J., Ismail, M. A. K., & Al-Subari, B. (2019, June). Strength and sulphate resistance of high performance concrete containing different fineness of Palm oil fuel ash. In *IOP Conference Series: Materials Science and Engineering* (Vol. 495, p. 012100). IOP Publishing.
- [3] Kamal, S. M., Saeed, J. A., & Mohammed, A. (2020). The characterization and modeling the mechanical properties of high strength concrete (HSC) modified with fly ash (FA). *Eng Technol J*, 38(2A), 173-184.
- [4] Burhan, L., Ghafor, K., & Mohammed, A. (2019). Modeling the effect of silica fume on the compressive, tensile strengths and durability of NSC and HSC in various strength ranges. *Journal of Building Pathology and Rehabilitation*, 4, 1-19.
- [5] Ali, B., Kurda, R., Herki, B., Alyousef, R., Mustafa, R., Mohammed, A., ... & Fayyaz Ul-Haq, M. (2020). Effect of varying steel fiber content on strength and permeability characteristics of high strength concrete with micro silica. *Materials*, 13(24), 5739.
- [6] Chindaprasirt, P., Chotetanorm, C., & Rukzon, S. (2011). Use of palm oil fuel ash to improve chloride and corrosion resistance of high-strength and high-workability concrete. *Journal of Materials in Civil Engineering*, 23(4), 499-503.
- [7] Alaskar, A., Albidah, A., Alqarni, A. S., Alyousef, R., & Mohammadhosseini, H. (2021). Performance evaluation of high-strength concrete reinforced with basalt fibers exposed to elevated temperatures. *Journal of Building Engineering*, 35, 102108.
- [8] Aldahdooh, M. A. A., Bunnori, N. M., & Johari, M. M. (2013). Development of green ultra-high performance fiber reinforced concrete containing ultrafine palm oil fuel ash. *Construction and Building Materials*, 48, 379-389.

- [9] Hussin, M. W., Ismail, M. A., Budiea, A., & Muthusamy, K. (2009). Durability of high strength concrete containing palm oil fuel ash of different fineness. *Malaysian Journal of Civil Engineering*, 21(2), 180-194.
- [10] Basiron, Y. (2007). Palm oil production through sustainable plantations. *European Journal of Lipid Science and Technology*, 109(4), 289-295.
- [11] Gibon, V., De Greyt, W., & Kellens, M. (2007). Palm oil refining. *European journal of lipid science and technology*, 109(4), 315-335.
- [12] Meijaard, E., Brooks, T. M., Carlson, K. M., Slade, E. M., Garcia-Ulloa, J., Gaveau, D. L., ... & Sheil, D. (2020). The environmental impacts of palm oil in context. *Nature plants*, 6(12), 1418-1426.
- [13] May, C. Y., & Nesaretnam, K. (2014). Research advancements in palm oil nutrition. *European journal of lipid science and technology*, 116(10), 1301-1315.
- [14] Mba, O. I., Dumont, M. J., & Ngadi, M. (2015). Palm oil: Processing, characterization and utilization in the food industry—A review. *Food bioscience*, 10, 26-41.
- [15] Maleka, A. M., Alkali, I. A., & Jaya, R. P. (2014). The indirect tensile strength of palm oil fuel ash (POFA) modified asphaltic concrete. *Applied mechanics and materials*, 587, 1270-1275.
- [16] Maclellan, M. (1983). Palm oil. *Journal of the American Oil Chemists' Society*, 60(2), 368-373.
- [17] Corley, R. H. V. (2009). How much palm oil do we need?. *Environmental Science & Policy*, 12(2), 134-139.
- [18] Tan, K. T., Lee, K. T., Mohamed, A. R., & Bhatia, S. (2009). Palm oil: Addressing issues and towards sustainable development. *Renewable and sustainable energy reviews*, 13(2), 420-427.
- [19] De Almeida, S. C., Belchior, C. R., Nascimento, M. V., dos SR Vieira, L., & Fleury, G. (2002). Performance of a diesel generator fuelled with palm oil. *Fuel*, 81(16), 2097-2102.
- [20] Hamada, H. M., Jokhio, G. A., Yahaya, F. M., & Humada, A. M. (2018, April). Properties of fresh and hardened sustainable concrete due to the use of palm oil fuel ash as cement replacement. In *IOP Conference Series: Materials Science and Engineering* (Vol. 342, p. 012035). IOP Publishing.
- [21] Mohammed, B. S., Al-Ganad, M. A., & Abdullahi, M. (2011). Analytical and experimental studies on composite slabs utilising palm oil clinker concrete. *Construction and Building Materials*, 25(8), 3550-3560.
- [22] Ibrahim, H. A., Razak, H. A., & Abutaha, F. (2017). Strength and abrasion resistance of palm oil clinker pervious concrete under different curing method. *Construction and Building Materials*, 147, 576-587.
- [23] Jagaba, A. H., Kutty, S. R. M., Hayder, G., Baloo, L., Noor, A., Yaro, N. S. A., ... & Usman, A. K. (2021). A systematic literature review on waste-to-resource potential of palm oil clinker for sustainable engineering and environmental applications. *Materials*, 14(16), 4456.
- [24] Ibrahim, H. A., & Razak, H. A. (2016). Effect of palm oil clinker incorporation on properties of pervious concrete. *Construction and Building Materials*, 115, 70-77.
- [25] Yap, S. P., Bu, C. H., Alengaram, U. J., Mo, K. H., & Jumaat, M. Z. (2014). Flexural toughness characteristics of steel-polypropylene hybrid fibre-reinforced oil palm shell concrete. *Materials & Design*, 57, 652-659.
- [26] Mohammadhosseini, H., Yatim, J. M., Sam, A. R. M., & Awal, A. A. (2017). Durability performance of green concrete composites containing waste carpet fibers and palm oil fuel ash. *Journal of cleaner production*, 144, 448-458.
- [27] Awal, A. A., & Mohammadhosseini, H. (2016). Green concrete production incorporating waste carpet fiber and palm oil fuel ash. *Journal of Cleaner Production*, 137, 157-166.
- [28] Tangchirapat, W., Khamklai, S., & Jaturapitakkul, C. (2012). Use of ground palm oil fuel ash to improve strength, sulfate resistance, and water permeability of concrete containing high amount of recycled concrete aggregates. *Materials & Design*, 41, 150-157.

- [29] Sofri, L. A., Mohd Zahid, M. Z. A., Isa, N. F., Azizi Azizan, M., Ahmad, M. M., Ab Manaf, M. B. H., ... & Ahmran, M. S. A. (2015). Performance of concrete by using palm oil fuel ash (POFA) as a cement replacement material. *Applied Mechanics and Materials*, 815, 29-33.
- [30] Oyejobi, D. O., Abdulkadir, T. S., & Ahmed, A. T. (2015). A study of partial replacement of cement with palm oil fuel ash in concrete production. *Journal of Agricultural Technology*, 12(4), 619-631.
- [31] Lim, S. K., Tan, C. S., Lim, O. Y., & Lee, Y. L. (2013). Fresh and hardened properties of lightweight foamed concrete with palm oil fuel ash as filler. *Construction and building materials*, 46, 39-47.
- [32] Khankhaje, E., Rafieizonooz, M., Salim, M. R., Khan, R., Mirza, J., & Siong, H. C. (2018). Sustainable clean pervious concrete pavement production incorporating palm oil fuel ash as cement replacement. *Journal of Cleaner Production*, 172, 1476-1485.
- [33] Munir, A. (2015). Utilization of palm oil fuel ash (POFA) in producing lightweight foamed concrete for non-structural building material. *Procedia Engineering*, 125, 739-746.
- [34] Sata, V., Jaturapitakkul, C., & Kiattikomol, K. (2004). Utilization of palm oil fuel ash in high-strength concrete. *Journal of Materials in Civil Engineering*, 16(6), 623-628.
- [35] Tangchirapat, W., Jaturapitakkul, C., & Chindaprasirt, P. (2009). Use of palm oil fuel ash as a supplementary cementitious material for producing high-strength concrete. *Construction and Building Materials*, 23(7), 2641-2646.
- [36] Johari, M. M., Zeyad, A. M., Bunnori, N. M., & Ariffin, K. S. (2012). Engineering and transport properties of high-strength green concrete containing high volume of ultrafine palm oil fuel ash. *Construction and Building Materials*, 30, 281-288.
- [37] Zeyad, A. M., Johari, M. A. M., Tayeh, B. A., & Yusuf, M. O. (2017). Pozzolanic reactivity of ultrafine palm oil fuel ash waste on strength and durability performances of high strength concrete. *Journal of Cleaner Production*, 144, 511-522.
- [38] Malkawi, A. B., Habib, M., Aladwan, J., & Alzubi, Y. (2020). Engineering properties of fibre reinforced lightweight geopolymer concrete using palm oil biowastes. *Australian Journal of Civil Engineering*, 18(1), 82-92.
- [39] Sumesh, M., Alengaram, U. J., Jumaat, M. Z., & Mo, K. H. (2019). Microstructural and strength characteristics of high-strength mortar using nontraditional supplementary cementitious materials. *Journal of Materials in Civil Engineering*, 31(4), 04019017.
- [40] Ahmad, S. A., & Rafiq, S. K. (2023). Numerical modeling to predict the impact of granular glass replacement on mechanical properties of mortar. *Asian Journal of Civil Engineering*, 1-19.
- [41] Ahmad, S. A., Rafiq, S. K., & Faraj, R. H. (2023). Modeling the compressive strength of green mortar modified with waste glass granules and fly ash using soft computing techniques. *Innovative Infrastructure Solutions*, 8(1), 67.
- [42] Ahmad, S. A., Ahmed, H. U., Rafiq, S. K., & Ahmad, D. A. (2023). Machine learning approach for predicting compressive strength in foam concrete under varying mix designs and curing periods. *Smart Construction and Sustainable Cities*, 1(1), 16.
- [43] Ahmad, S. A., Rafiq, S. K., Hilmi, H. D. M., & Ahmed, H. U. (2023). Mathematical modeling techniques to predict the compressive strength of pervious concrete modified with waste glass powders. *Asian Journal of Civil Engineering*, 1-13.
- [44] Ahmad, S. A., Rafiq, S. K., Ahmed, H. U., Abdulrahman, A. S., & Ramezaniyanpour, A. M. (2023). Innovative soft computing techniques including artificial neural network and nonlinear regression models to predict the compressive strength of environmentally friendly concrete incorporating waste glass powder. *Innovative Infrastructure Solutions*, 8(4), 119.